Double nerve transfer to a single target muscle: experimental model in the upper extremity

Matthias Luft[1,2], Johanna Klepetko[1,2], Silvia Muceli[3], Jaime Ibáñez[4,5], Vlad Tereshenko[1,2], Christopher Festin[1,2], Gregor Längle[1,2], Olga Politikou[1,2], Udo Maierhofer[1,2], Dario Farina[4], Oskar C. Aszmann[1,6], Konstantin D. Bergmeister[1,2,7]

[1]Clinical Laboratory for Bionic Extremity Reconstruction, Department of Plastic, Reconstructive and Aesthetic Surgery, Medical University of Vienna, Vienna, Austria

[2]Center for Biomedical Research, Medical University of Vienna, Vienna, Austria

[3]Department of Electrical Engineering, Chalmers University of Technology, Gothenburg, Sweden

[4]Department of Bioengineering, Imperial College London, London, UK

[5]Department of Clinical and Movement Neuroscience, University College London, London, UK

[6]Department of Plastic, Reconstructive and Aesthetic Surgery, Medical University of Vienna, Vienna, Austria

[7]Karl Landsteiner University of Health Sciences, Department of Plastic, Aesthetic and Reconstructive Surgery, University Hospital St. Poelten, Krems, Austria

*** Correspondence:**

Konstantin Bergmeister, MD PhD

Clinical Laboratory for Bionic Extremity Reconstruction,

Department of Plastic, Reconstructive and Aesthetic Surgery

Medical University of Vienna

Waehringer Guertel 18-20

A-1090 Vienna, Austria

kbergmeister@gmail.com

Keywords: nerve injury, peripheral nerve, nerve transfer, targeted muscle reinnervation, rat model, microsurgery

Abstract

Surgical nerve transfers are used to efficiently treat peripheral nerve injuries, neuromas, phantom limb pain or improve bionic prosthetic control. Commonly, one donor nerve is transferred to one target muscle. However, the transfer of multiple nerves onto a single target muscle may increase the number of muscle signals for myoelectric prosthetic control and facilitate the treatment of multiple neuromas. Currently, no experimental models are available for multiple nerve transfers to a common target muscle in the upper extremity. This study describes a novel experimental model to investigate the neurophysiological effects of peripheral double nerve transfers. For this purpose, we developed a forelimb model to enable tension-free transfer of one or two donor nerves in the upper extremity. Anatomic dissections were performed to design the double nerve transfer model (n=8). In 62 male Sprague-Dawley rats the ulnar nerve of the antebrachium alone (n=30) or together with the anterior interosseus nerve (n=32) was transferred to reinnervate the long head of the biceps brachii. Before neurotization, the motor branch to the biceps' long head was transected at the motor entry point and resected up to its original branch to prevent auto-reinnervation. In all animals, coaptation of both nerves to the motor entry point could be performed tension-free. Mean duration of the procedure was 49 ± 13 min for the single nerve transfer and 78 ± 20 min for the double nerve transfer. Twelve weeks after surgery, muscle response to neurotomy, behavioral testing, retrograde labeling and structural analyses were performed to assess reinnervation. These analyses indicated that all nerves successfully reinnervated the target muscle. No aberrant reinnervation was observed by the originally innervating nerve. Our observations suggest a minimal burden for the animal with no signs of functional deficit in daily activities or auto-mutilation in both procedures. Furthermore, standard neurophysiological analyses for nerve and muscle regeneration were applicable. This newly developed nerve transfer model allows for the reliable and standardized investigation of neural and functional changes following the transfer of multiple donor nerves to one target muscle.

1 Introduction

Nerve transfers offer a variety of therapeutic possibilities in modern extremity reconstruction, such as treating peripheral nerve injuries, neuromas, phantom limb pain, improving prosthetic control or restoring function following spinal cord injuries (Aszmann et al., 2015;Farina et al., 2017;Dumanian et al., 2019;Van Zyl et al., 2019). Compared to conventional nerve repair modalities, nerve transfers are capable of bypassing slow peripheral nerve regeneration (Terzis and Papakonstantinou, 2000), thus preventing irreversible muscle fibrosis before reinnervation (Mackinnon and Novak, 1999). For this purpose, nearby nerves with a sufficient axonal load and lesser functional importance are neurotomized and transferred to the injured nerve (Oberlin et al., 1994;Bertelli et al., 1997). Because of overall faster regeneration and better functional outcomes compared to nerve grafting, this surgical procedure has been able to improve the devastating effects of peripheral nerve and brachial plexus lesions, which have otherwise often led to long-term health impairment and subsequent socioeconomic costs (Mackinnon and Novak, 1999;Terzis and Papakonstantinou, 2000;Bergmeister et al., 2020). Additionally, they are used in a procedure termed targeted muscle reinnervation (TMR) to improve myoelectric prosthetic control (Kuiken et al., 2009;Kapelner et al., 2016), treat neuromas or phantom limb pain (Mioton et al., 2020). Here, amputated nerves within an extremity stump are transferred to residual stump muscles, thus significantly improving the recording of neural activity about motor intent and the control of myoelectric prostheses. Generally, one donor nerve is transferred to one target muscle head and this concept has been well studied with high clinical success (Kuiken et al., 2009;Aszmann et al., 2015;Farina et al., 2017). However, the use of multiple nerve transfers to a single target muscle head may provide additional benefits for these clinical indications but has not been clinically explored. Although several nerve transfer models have been established (Kuiken et al., 1995;Bergmeister et al., 2016;Aman et al., 2019), none of them has investigated multiple peripheral nerve transfers in the upper extremity. Only one model where multiple donor nerves are used to restore muscle function in the rat hindlimb has been described (Kuiken et al., 1995). However, as most nerve

injuries occur in the upper extremity, an upper extremity model for experimental investigation of this concept is needed (Scholz et al., 2009).

In this study, we propose a surgical nerve transfer model to allow the transfer of multiple donor nerves to a single muscle head and we validate this model in the rat forelimb. This model allows for reliable analyses with all standard neurophysiological investigations of the motor unit for possible implementation of this concept to clinical application.

2 Materials and methods

2.1 Experimental design

Eight rat cadavers were dissected to design the double nerve transfer procedure. An important criterion for the selection of the donor nerves and the target muscle was clinical relevance. First, eligible peripheral motor nerves were determined for a reliable, tension-free transfer to the long head of the biceps muscle. Then, the topographical relationships between the biceps' long head, its motor nerve branch, the ulnar nerve in the antebrachium (UN) and the anterior interosseus nerve (AIN) were studied and subsequently compared to the human anatomy. These studies verified the anatomical feasibility of transferring both the distal UN and AIN to the long head of the biceps.

Sixty-two Sprague-Dawley rats aged 8-10 weeks were randomly allocated into two groups by an animal care taker to investigate functional and structural changes following single (SNT) and double nerve transfer (DNT). Thirty-two animals were assigned to the DNT group (Figure 1), while 30 animals underwent the single nerve transfer of the UN and were used as control (Figure 1). Twelve weeks after surgery, microscopic inspection of the motor entry point (n=62), nerve crush and neurotomy (n=32), and Terzis' grooming test (n=51) (Inciong et al., 2000) were performed. After the final functional assessments, muscle specimens were harvested and weighed (n=32). Thirty-eight animals were assigned for retrograde labeling analyses. Sample size calculations performed by a biostatistician were

considered in the planning of the studies. Planning, conducting and reporting of experiments were performed according to the ARRIVE (Animal Research: Reporting of In Vivo Experiments) guidelines (Percie Du Sert et al., 2020). The protocols for these experiments were approved by the ethics committee of the Medical University of Vienna and the Austrian Ministry for Research and Science (reference number BMBWF- 66.009/0413-V/3b/2019) and strictly followed the principles of laboratory animal care as recommended by the Federation of European Laboratory Animal Science Associations (FELASA)(Guillen, 2012).

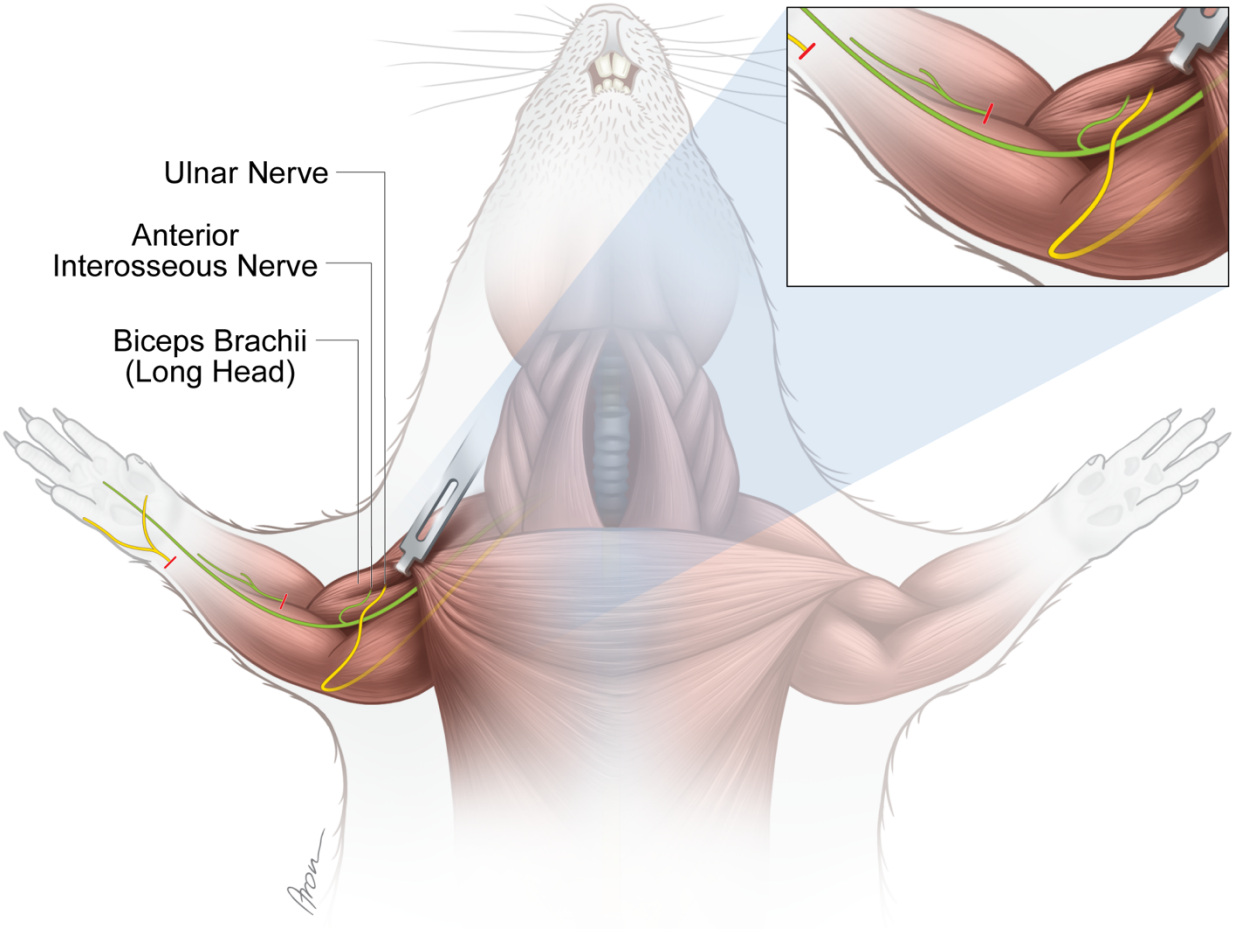

Figure 1. **Experimental nerve transfer models**. *Single-nerve transfer model:* The UN (yellow) was transected distally to the palmar cutaneous branch in the forearm and surgically transferred to reinnervate the long head of the biceps (n=30). *Multiple-nerve transfer model:* Both the UN (yellow) and AIN (green) were redirected to reinnervate the long head of the biceps (n=32). Before both nerve transfer procedures, the originally innervating branch of the MCN was removed. The

untreated contralateral biceps muscles served as internal control for both groups. The red lines indicate the level of transection. Credit: Aron Cserveny.

2.2 Nerve transfer model

For each procedure, anesthesia was induced with ketamine (100 mg/kg) and xylazine (5 mg/kg) intraperitoneally and maintained by volume-controlled ventilation (40% O2, room air, 1.5-2% isoflurane) following orotracheal intubation. Piritramide (0.3 mg/kg) was administered subcutaneously for analgesia. Furthermore, the drinking water was mixed with piritramide and glucose (30 mg piritramide and 30 ml 10% glucose dissolved in 250 ml drinking water) and administered ad libitum for pain relief during the first seven postoperative days. After the experimental tests, animals were euthanized with a lethal dose of pentobarbital (300 mg/kg) injected intracardially under deep anesthesia. All animals were examined daily by an animal keeper for pain, sensory deficits, impairments in daily activities, wound dehiscence and infection. All nerve transfer procedures were performed by the same surgeon and assistant.

2.2.1 Single nerve transfer

A lazy S-shaped incision was made from 5 mm caudal to the greater tubercle of the humerus over the medial epicondyle along the ulnar side of the forearm until 5 mm proximal to the forepaw (Figure 2A). Following the dissection of the subcutaneous tissue, the antebrachial fascia was opened through an incision placed over the palmaris longus muscle to preserve the underlying ulnar collateral vessels. Then, the flexor carpi ulnaris muscle was bluntly mobilized and retracted ulnarly using a Magnetic Fixator Retraction System (Fine Science Tools, Heidelberg, Germany) to expose the UN. Further exposure of the dorsal and palmar cutaneous branches of the UN was carried out using an operating microscope (Carl Zeiss, Munich, Germany) (Figure 2B). The palmar branch was cut right after its emergence and the UN was subsequently transected as distally as possible. The UN was dissected proximally to its distal exit from the cubital tunnel while preserving the ulnar artery and basilic vein.

Intraneural dissection allowed for conservation of the dorsal cutaneous and flexor carpi ulnaris motor branches (Figure 2B), while facilitating a tension-free nerve coaptation. Next, the incision of the antebrachial fascia was extended proximally to open the brachial fascia above the cubital fossa and biceps. Subsequently, the pectoral muscles were retracted to expose the musculocutaneous nerve's (MCN) branch to the long head of the biceps running along the bicipital groove (Figure 2C). The motor branch of the MCN to the biceps' long head was then cut at the motor insertion point and the proximal segment subsequently removed from its division to prevent spontaneous regeneration. Next, the UN was routed proximally over the cubital fossa and coapted tension-free to the epimysium near the original motor insertion point with one 11-0 (Ethilon, Ethicon, Johnson & Johnson Medical Care, USA) simple interrupted stitch (Figure 2D).

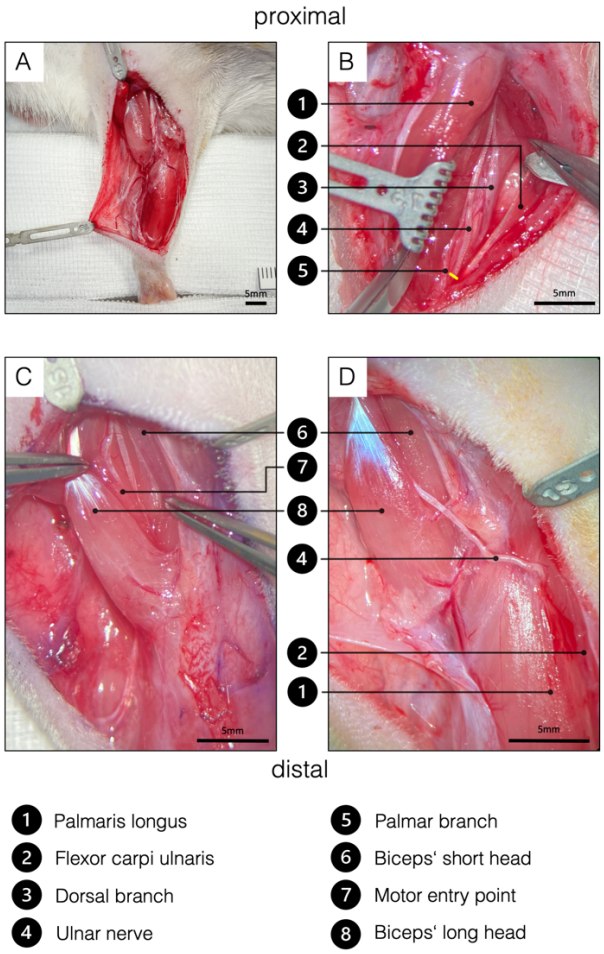

153

154 **Figure 2**. **Surgical procedure of the ulnar nerve transfer.** (**A**) Overview of the rats' supinated right forelimb after the
155 brachial and antebrachial fascia were removed. (**B**) Two blunt retractors have been placed to pull the flexor carpi ulnaris
156 and the palmaris longus apart, revealing the underlying UN. The yellow line indicates the level of transection to gain
157 sufficient length to reach the biceps' long head tension-free. To achieve this, the palmar cutaneous branch must be
158 transected, while the dorsal cutaneous branch can be preserved. (**C**) For better visualization, the brachial fascia was opened
159 above the biceps. A sharp retractor was placed to pull back the pectoral muscles and thus revealed the two biceps heads,
160 which were bluntly separated. In the deep bicipital groove, the MCN and its motor branch to the long head of the biceps
161 were identified. Maximum length of the motor branch to the long head was removed to prevent spontaneous regeneration.
162 (**D**) Eventually, the UN was rerouted from between the palmaris longus and flexor carpi ulnaris to the long head of the
163 biceps and sutured to the epimysium at the former original motor entry point. This procedure on the one hand spares the
164 denervation of the flexor carpi ulnaris and the flexor digitorum superficialis and the invasive dissection through the cubital
165 tunnel.

2.2.2 Double nerve transfer

The skin incision, exposure of the distal UN as well as the denervation of the biceps' long head were performed as described in the single nerve transfer. Before coaptation of the UN, the median nerve and AIN were dissected. For better exposure of the AIN, one blunt retractor was carefully placed to pull the proximal belly of the pronator teres muscle ulnarly (Figure 3A). After identifying the AIN, it was transected and dissected proximally in an intraneural fashion to its branching point (Figure 3A). Then, both the UN and the AIN were neurotized to the epimysium near the original motor insertion point with one 11-0 (Ethilon, Ethicon, Johnson & Johnson Medical Care) simple interrupted stitch each (Figure 3B). Significant caliber differences between the motor branch of the biceps' long head and the two transferred nerves required neurotization directly to the epimysium. In this way, the regeneration distance was kept as short as possible, hence minimizing the reinnervation time. It is particularly important not to place the two nerves in direct proximity in the tissue (Figure 3B) as this increases the complexity of the dissection and therefore the risk of injuring the nerves in the follow-up examinations. Wound closure was performed with fascial and deep dermal 6-0 (Vicryl, Ethicon, Johnson and Johnson Medical Care, Austria) simple interrupted sutures followed by running subcuticular suture with 6-0 (Vicryl, Ethicon, Johnson and Johnson Medical Care, Austria).

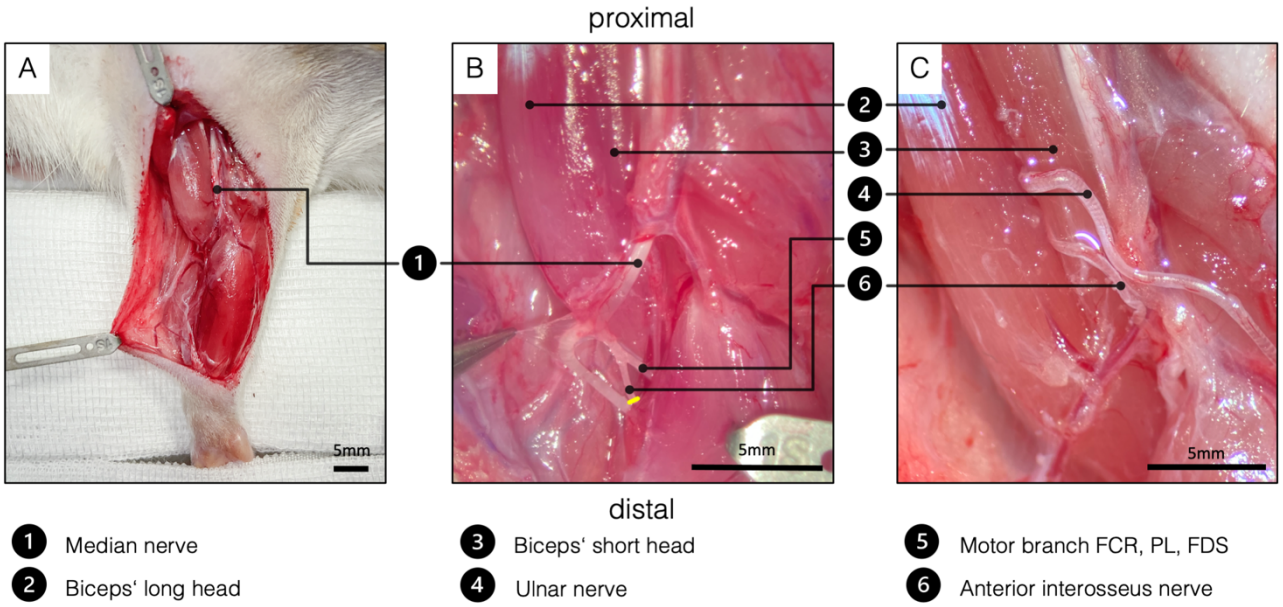

Figure 3. Surgical procedure of the double nerve transfer. (A) General view of the right supinated forelimb. The proximal hook pulls the pectoral muscles towards proximal for better presentation. (B) The brachial and antebrachial fascia and the motor branch to the pronator teres muscle were removed for better visualization. In the cubital fossa, three branches arise from the median nerve: one muscle branch supplying the pronator teres (resected), one muscle branch supplying the flexor carpi radialis, palmaris longus and flexor digitorum superficialis and the AIN supplying pronator quadratus, flexor pollicis longus and flexor digitorum profundus. After transecting the AIN (yellow line), proximal dissection in an intraneural fashion gains sufficient length to reach the biceps' motor entry point. (C) Surgical site before wound closure, after both the UN and the AIN were transferred to the physiological motor entry point of the long head of the biceps. (FCR - flexor carpi radialis. PL - palmaris longus. FDS - flexor digitorum superficialis).

2.3 Behavioral evaluation

Quantitative assessment of grooming behavior was carried out and filmed twelve weeks after the single (n=21) and double nerve transfer (n=30) using Terzis' grooming test (Inciong et al., 2000), a modification of Bertelli's grooming test (Bertelli and Mira, 1993). To keep the animals' stress level at a minimum, testing was performed in the animals' familiar environment. In brief, 1 to 3 ml of water was sprinkled on the rats' snouts, which led to consistent bilateral grooming movements of the forelimbs. Grading of the grooming performance was assessed by the following score: grade 1, paws

reach mouth or elbow is extended; grade 2, paws reach mouth and beneath eyes; grade 3, paws reach eyes; grade 4, paws reach between eyes and ears; grade 5, paws reach behind the ears. The slow-motion video sequences were graded by a blinded observer.

2.4 Retrograde labeling

Assessment of the motor unit at the spinal cord level after nerve transfer surgery was performed via retrograde labeling as previously described (Hayashi et al., 2007). In brief, retrograde tracers are taken up by terminal axons and transported via retrograde axonal transport to label the cell somas in the spinal cords' ventral root. In eight additional untreated control animals both the UN in the antebrachium and the AIN were transected and placed into conduit reservoirs for one hour, either filled with 5 µl of 10% Fluoro-Ruby (Invitrogen, Carlsbad, CA, USA) or 5 µl of 2% Fast-Blue (Polysciences, Warrington, PA, USA). Tracer leakage was prevented by sealing the reservoir around the nerve with Vaseline (Vaselinum album, Fagron, Glinde, Germany). Hence, the corresponding motor neuron pools in the spinal cord (C8-Th1) were localized (Figure 4). To further prevent bias due to differences in penetration of the tracers, the nerves were alternately colored with Fluoro-Ruby and Fast-Blue. Additionally, twelve weeks following the SNT (n=15) and DNT (n=15) surgery, motor neurons reinnervating the long head of the biceps were studied. Through a 15mm incision above the biceps, the biceps' long head and its insertion site were exposed. A Hamilton micro syringe was then used to inject 10µl 2% Fluoro-Gold (Fluorochrome, LLC, Denver, CO) evenly into the biceps' long head near the motor insertion site. After tracer injection with a small gauge needle, the syringe was kept inside the muscle for one minute before slowly withdrawing it to keep leakage to a minimum. Seven days following retrograde labeling, the animals were deeply anesthetized by a lethal dose of xylazine, ketamine and pentobarbital intraperitoneally before the left ventricle was perfused with 400ml of 0.9% NaCl followed by 400ml of 4% paraformaldehyde (PFA) solution. Then, the spinal cord segments C4-Th2 were harvested and stored in 4% PFA for 24 hours at +4°, followed by 24h in 0.1M phosphate

buffered saline PBS at +4°. Then, the specimens were dehydrated in a PBS solution with increasing sucrose concentrations of 10%, 25% and 40% for 24 hours each before embedding them in Tissue-Tek® O.C.T.™ Compound (Sakura Finetek Europe B.V., Alphen aan den Rijn, Netherlands). Spinal cord segments were cut longitudinally into 40-µm sections using a cryostat (Leica, Germany). To assess the reinnervation, each spinal cord section was analyzed in an observer blinded setting using a fluorescence microscope (Carl Zeiss, Munich, Germany). Spinal cord segments of labeled motor neurons after DNT (Fluoro-Gold) were compared to the double labeled (Fast-Blue, Fluoro-Ruby) segments of the untreated animals.

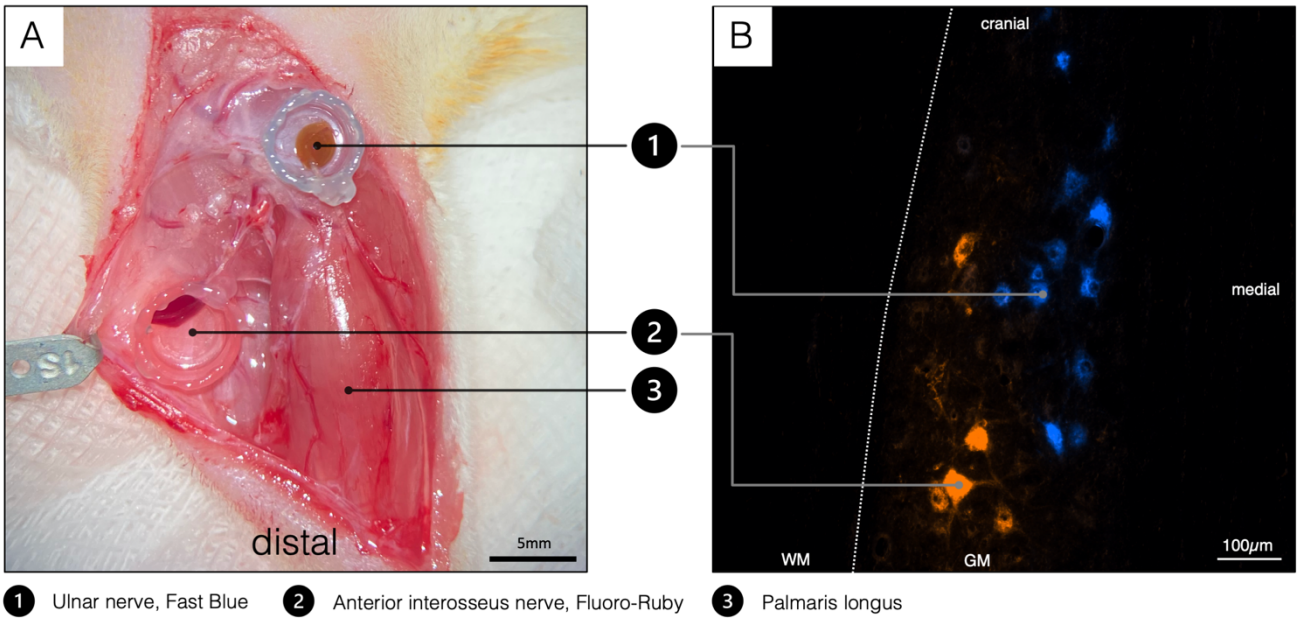

Figure 4. Double retrograde labeling. (A) The selected donor nerves were both dissected in a right forelimb and placed in a conduit reservoir filled with Fast-Blue (UN) and Fluoro-Ruby (AIN) respectively for one hour. Wet sterile swabs were placed above the surgical site to prevent the tissue from drying and the fluorescent dyes from bleaching. (B) Spinal cord section C8-Th1. Labeled AIN (orange) and UN motoneuron pool (blue). WM – white matter, GM – grey matter.

2.5 Neuromuscular analyses

The lengths of both the UN (n=6) and AIN (n=6) were measured intraoperatively before coaptation to the muscle. Twelve weeks following surgery, the motor entry point was microscopically examined for

proper reinnervation and neuroma formation in all animals. Muscle reaction to nerve crush (see Video 2 for muscle reaction to MCN crush in the control side) and neurotomy was assessed in animals following DNT (n=17) and compared to animals following SNT (n=15). For internal control, the motor branches to the biceps' long head were crushed and neurotomized in the contralateral forelimbs. Conclusively, to assess neuromuscular regeneration after denervation, the biceps muscles were resected and weighed immediately after removal using a microscale.

2.6 Statistical analysis

An ANCOVA was conducted to determine effects of the nerve transfer procedure (SNT and DNT) on the reinnervated muscle mass after adjusting for control muscle mass. In addition, a paired-samples t-test was used to determine whether there was a change of muscle mass following SNT or DNT between the two sides. All data analyses were performed using SPSS Statistics for Macintosh, Version 25.0 (IBM, Armonk, New York, USA).

3 Results

3.1 Nerve transfer surgery

All animals survived the surgical nerve transfers and showed normal gait and grasping behavior in the twelve-week follow-up period. All animals were able to carry out activities of daily behavior unhindered and no signs of severe pain, wound dehiscence, auto-mutilation or infection were documented. Mean surgery time was 49 ± 13 min for the SNT procedures and 78 ± 20 min for the DNT procedures.

3.2 Behavioral evaluation

Slow motion video sequence analysis by a blinded evaluator showed that twelve weeks following the SNT and DNT, all animals could consistently reach behind their ears and therefore achieved a maximum score of 5 (Video 1).

3.3 Retrograde Labeling

Analyses of the spinal cord following UN transfer showed adequate motor neuron staining in the corresponding segments (Th1-C8). When comparing the spinal cords of the untreated animals with spinal cords of animals which underwent DNT, the distribution pattern of the longitudinally arranged Fluoro-Gold dyed clusters provides strong evidence that both the UN and AIN innervated the biceps' long head (see Figure 4 for a representative example). Furthermore, no signs of spontaneous regeneration from the MCN were noted by analyzing the corresponding spinal cord segments (C5-C7).

3.4 Neuromuscular analyses

Both the donor nerve branches, and biceps' motor entry point were topographically consistent. The UN measured a mean length of 23.08 ± 1.36 mm from the distal exit of the cubital tunnel to the distal stump. The AIN transfer provided a mean length of 10.50 ± 1.61 mm measured from its branching off the median nerve to the distal stump.

Twelve weeks following nerve transfer surgeries, macroscopic examination of all biceps motor entry points showed successful reinnervation but no auto-innervation by the MCN and no signs of neuroma were detected. Adequate muscle fibrillation was observed in all animals upon crushing and neurotomizing the donor nerves individually following SNT and DNT (UN crush and AIN crush response is shown in video 3 and 4 respectively).

3.4.1 Comparison of reinnervated muscle mass

There was a linear relationship between treated and untreated muscle mass for each nerve transfer procedure, as assessed by visual inspection of a scatterplot. There was homogeneity of regression

slopes as the interaction term was not statistically significant, $F(1, 28) = .238$, $p = .630$. Standardized residuals for the interventions and for the overall model were normally distributed, as assessed by Shapiro-Wilk's test ($p > .05$). There was homoscedasticity and homogeneity of variances, as assessed by visual inspection of a scatterplot and Levene's test of homogeneity of variance ($p = .504$), respectively. There were no outliers in the data, as no cases were detected with standardized residuals greater than ± 3 standard deviations.

After adjustment for control muscle mass, there was a statistically significant difference in muscle mass between the treated sides following SNT and DNT, $F(1, 29) = 24.030$, ***$p < .001$, partial $\eta^2 = .453$. Muscle mass was statistically significantly larger in the DNT group (303.01 ± 7.76 mg) compared to the SNT group (245.57 ± 8.29 mg), with a mean difference of 57.45 (95% CI, 33.48 to 81.41) mg, ***$p < .001$. Data are reported adjusted mean ± standard error.

3.4.2 Comparison of reinnervated and control muscle mass

No outliers were detected as assessed by inspection of a boxplot. The assumption of normality was not violated, as assessed by Shapiro-Wilk's test for the SNT ($p = .758$) and DNT group ($p = .307$).

The mean muscle mass was reduced following SNT (235.07 ± 44.05 mg) as opposed to the untreated contralateral side (292.93 ± 35.17 mg) with a statistically significant decrease of -57.87 (95% CI, -77.38 to -38.35) mg, $t(14) = -6.360$, ***$p < .001$, $d = 1.64$. However, mean muscle mass following DNT (312.28 ± 37.74 mg) compared to the untreated contralateral side (315.97 ± 28.22 mg) was similar and showed no statistically significant change ($p = .571$). Data are reported as mean ± standard deviation.

4 Discussion

The present study provides a robust and easily accessible model for surgical double nerve transfers to a single target muscle in the rat's upper extremity. We offer detailed step-by-step instructions on how to reproduce this model, including potential pitfalls. For comparison, the model also offers a

307 description of a single nerve transfer to the same target muscle. We employed nerve crush, neurotomy,
308 behavioral analysis and retrograde labeling which indicated that neuromuscular regeneration of two
309 donor nerves occurred into one target muscle.
310 To our knowledge, only one rat model for multiple peripheral innervation of a single target has been
311 described. However, that previous model was for the lower extremity and did not provide detailed
312 description for step by step reproduction of the model (Kuiken et al., 1995). Hindlimb models do not
313 adequately represent the physiology of upper extremity nerve transfers and targeted muscle
314 reinnervation procedures. This notion is supported by the clinical discrepancy between the excellent
315 outcomes for upper extremity compared to the poor outcomes for lower extremity nerve transfers (Ray
316 et al., 2016). Furthermore, most nerve transfers are currently conducted in the upper extremity for both
317 nerve reconstruction and prosthetic control. We already established single peripheral nerve transfer
318 models in the upper extremity (Bergmeister et al., 2016;Aman et al., 2019), which were considered for
319 developing this novel model. For this purpose, we conducted anatomical dissections in eight rat
320 cadavers to design the DNT concept to allow tension-free approximation of the two motor nerves to
321 the target biceps muscle. Theoretically, many other target muscles are also feasible due to the sufficient
322 length of both the UN and AIN. However, the biceps muscle provides an optimal target that is
323 accessible for all standard structural and functional analyses and accurately represents a surgical target
324 in clinical nerve transfer scenarios as well.
325 The implementation of this model requires an operating microscope, a set of microsurgery tools and
326 advanced microsurgical skills to achieve reproducible results. In our experience, dissection of the UN
327 in the antebrachium can be performed in a straightforward manner and preservation of the motor branch
328 to the flexor carpi ulnaris muscle, the dorsal sensory branch and the ulnar artery is easily feasible.
329 Subsequently, transecting the UN as distally as possible allows for tension-free coaptation to the
330 proximal target muscle. Exposure of the MCN's motor branch to the long head of the biceps is best
331 achieved in the bicipital groove by retracting the overlaying pectoral muscles medially. Here,

considerable care must be taken when dividing the two bicep heads to preserve the bicipital artery, which enters the long head in the distal portion and advances in proximal direction. Injury to this vessel has shown to affect functional measures in previous experiments. Another hazard in the DNT model is potential injury of the median vessels in the cubital fossa. To prevent this scenario, special attention is required during the dissection of the median nerve, because the median vessels are either found directly beneath or above the nerve. It is mandatory to dissect the AIN intraneurally to its proximal branching point to enable tension-free coaptation to the original motor point of the biceps. Due to the target to donor nerve diameter discrepancies, we chose to suture the donor nerves to the motor entry point epimysially. In previous models, this approach led to reliable reinnervation of the target muscle (Bergmeister et al., 2019).

Our behavioral observations indicate that the procedures did not cause extraordinary distress or pain under adequate analgesia postoperatively. As early as one week after surgery, behavioral testing was carried out in randomly selected individual animals, and all of them achieved the maximum score. Likewise, after a 12-week regeneration period, all animals from both the control and the experimental DNT group achieved the maximum score of Terzis grooming test (Inciong et al., 2000) (Video 1). Hence, it seems that two motor nerves of different origin governing the same muscle did not hamper activities of daily living. Additionally, no substantial pain or neuroma pain was evident. When comparing the two procedures, it takes only marginally longer to perform the DNT, while no additional physical stress or motor deficits were observed postoperatively.

The donor nerves reinnervated the target muscle within 12 weeks in all animals as indicated macroscopically during dissection and by the fact that nerve crush or neurotomy induced fasciculations of the muscle (Videos 3 and 4). Likewise, intramuscular retrograde labeling showed the uptake and transport of tracer dye into the motor neuron columns of the two transferred nerves.

Interestingly, after 12 weeks, muscle mass of the UN reinnervated muscles only recovered to 80.25 % of the contralateral side. This is in contrast with previous studies performed by authors of this work

(Bergmeister et al., 2019). A possible explanation for this mismatch is the difference of the levels at which the UN was cut and transferred in the two studies. Unlike in the previous study where the entire UN was transferred, here the UN was transferred at the wrist level. This may have caused that the donor nerve was not able to fully regenerate the long head of the biceps due to the lower motor axon numbers. Detailed analyses exist for humans, where the UN at wrist level only contains 1226 ± 243 motor axons compared to the entire UN (2670 ± 347) whereas the MCN contains 1601 ± 164 (Gesslbauer et al., 2017). Considering that the muscle mass of double reinnervated muscles regenerated to 98.83%, it appears that the two donor nerves were better able to reinnervate and adequately restore 24.72 % more muscle mass than the SNT. This additionally indicates that both SNT and DNT procedures were successful and that DNT with a high axonal load may lead to higher muscle reinnervation and functional regeneration.

Previous findings (Bergmeister et al., 2019) reported neuroma formation at the insertion point following nerve transfer. These consisted presumably mainly of sensory axons and the surplus of motor neurons which was not able to innervate motor endplates. We did not observe neuroma formation in this study and believe, that this is because the donor nerves comprised only few sensory axons and the donor-to-recipient ratio of motor axons and targets was more balanced than in the previous study, as mentioned above. Therefore, we assume that no fibers were lost at the insertion site to the muscle, which may have formed a neuroma. Although the question of the optimal donor-to-recipient ratio for optimal outcome remains unsolved, further investigations in this surgical model are ongoing to answer this question and contribute to surgical refinement of nerve transfers.

One potential limitation of this study is the use of the mixed UN containing both sensory and motor nerve fibers. For better outcomes of surgical nerve transfers, “pure” motor nerves should be preferred, such as the AIN used here, to avoid sensory to motor axon incongruence (Ray et al., 2016). We decided to transfer the UN at a level, where it also contains sensory fibers of the superficial branch because unlike in human, intraneural fascicular dissection to identify the two branches proximal to Guyon’s

canal is impossible due to intermingling axons at the level of Guyon's canal. Uncomplicated dissection, significant transfer leeway and the lack of a better alternatives made the UN the best option.

The presented nerve transfer model finds broad application in many research fields. It offers the possibility to investigate basic neurophysiology, but also clinical applications of surgical nerve transfers for biological reconstruction and bionic reconstruction via targeted muscle reinnervation. After amputation, targeted muscle reinnervation can create additional myosignals to improve basic prosthetic control. In TMR, neuromas within the stump are cut and the healthy fascicles are then transferred to intact muscle segments, after denervation from their original innervation. EMG technology can record and decipher neuronal signals from those reinnervated areas into signals for prosthetic movement (Bergmeister et al., 2017;Muceli et al., 2019b;Salminger et al., 2019). The biceps' long head is suitable to perform various EMG examinations, as we have previously shown (Bergmeister et al., 2019;Muceli et al., 2019a). Especially with novel multichannel EMG technology (Muceli et al., 2015), individual motor unit action potentials can potentially be decoded from such signals as we have previously shown in SNT models (Muceli et al., 2019a).

In conclusion, this study demonstrated that a single target muscle can host two separate donor nerves. Our results suggest that both the SNT and DNT models are suitable for common neurophysiological examinations in peripheral nerve research. The concept of transferring multiple nerves to a single target may improve muscle reinnervation, prosthetic interfacing, neuroma therapy or facilitate phantom limb pain management. Until first clinical applications can be translated, further research is needed to fully understand the neurophysiological changes following multiple nerve transfers.

5 Conflict of Interest

All authors declare that they have no competing interest. The ERC had no influence on the study.

6 Author Contributions

Conception and design: ML, JK, SM, JI, VT, CF, GL, OP, UM, DF, OCA and KDB. Analyses and interpretation of data: ML, JK, SM, JI, VT, CF, GL, OP, UM, DF, OCA and KDB. Drafting of the article: ML, SM, DF, OCA, and KDB. Critical revision for important intellectual content and final approval of the version to be published: all authors.

7 Funding

This project has received funding from the European Research Council (ERC) under the European Union's Horizon 2020 research and innovation program (grant agreement No 810346).

8 Abbreviations

AIN	Anterior interosseus nerve
DNT	Double nerve transfer
EMG	Electromyography
MCN	Musculocutaneous nerve
SNT	Single nerve transfer
TMR	Targeted muscle reinnervation
UN	Ulnar nerve

9 Acknowledgments

We thank AM. Willensdorfer for her continuous technical assistance and A. Cserveny for his admirable illustrations in this project. In addition, we thank Florian Frommlet for his statistical analyses and expertise as a biostatistician.

10 Data availability

The following dataset was generated:

Luft et al. (2021), Muscle mass of the long head of the biceps following single and double nerve transfer, Dryad, Dataset, https://doi.org/10.5061/dryad.3j9kd51jb

11 References

Aman, M., Sporer, M., Bergmeister, K., and Aszmann, O. (2019). Experimentelle Modelle für selektive Nerventransfers der oberen Extremität: Modellbeschreibung und neurophysiologische Effekte. *Handchirurgie · Mikrochirurgie · Plastische Chirurgie* 51**,** 319-326.

Aszmann, O.C., Roche, A.D., Salminger, S., Paternostro-Sluga, T., Herceg, M., Sturma, A., Hofer, C., and Farina, D. (2015). Bionic reconstruction to restore hand function after brachial plexus injury: a case series of three patients. *Lancet* 385**,** 2183-2189.

Bergmeister, K.D., Aman, M., Muceli, S., Vujaklija, I., Manzano-Szalai, K., Unger, E., Byrne, R.A., Scheinecker, C., Riedl, O., Salminger, S., Frommlet, F., Borschel, G.H., Farina, D., and Aszmann, O.C. (2019). Peripheral nerve transfers change target muscle structure and function. *Sci Adv* 5**,** eaau2956.

Bergmeister, K.D., Aman, M., Riedl, O., Manzano-Szalai, K., Sporer, M.E., Salminger, S., and Aszmann, O.C. (2016). Experimental nerve transfer model in the rat forelimb. *European Surgery* 48**,** 334-341.

Bergmeister, K.D., Große-Hartlage, L., Daeschler, S.C., Rhodius, P., Böcker, A., Beyersdorff, M., Kern, A.O., Kneser, U., and Harhaus, L. (2020). Acute and long-term costs of 268 peripheral nerve injuries in the upper extremity. *PLOS ONE* 15**,** e0229530.

Bergmeister, K.D., Vujaklija, I., Muceli, S., Sturma, A., Hruby, L.A., Prahm, C., Riedl, O., Salminger, S., Manzano-Szalai, K., Aman, M., Russold, M.-F., Hofer, C., Principe, J., Farina, D., and Aszmann, O.C. (2017). Broadband Prosthetic Interfaces: Combining Nerve Transfers and Implantable Multichannel EMG Technology to Decode Spinal Motor Neuron Activity. *Frontiers in Neuroscience* 11.

Bertelli, J.A., and Mira, J.C. (1993). Behavioral evaluating methods in the objective clinical assessment of motor function after experimental brachial plexus reconstruction in the rat. *J Neurosci Methods* 46**,** 203-208.

Bertelli, J.A., Mira, J.C., Pecot-Dechavassine, M., and Sebille, A. (1997). Selective motor hyperreinnervation using motor rootlet transfer: an experimental study in rat brachial plexus. *J Neurosurg* 87**,** 79-84.

Dumanian, G.A., Potter, B.K., Mioton, L.M., Ko, J.H., Cheesborough, J.E., Souza, J.M., Ertl, W.J., Tintle, S.M., Nanos, G.P., Valerio, I.L., Kuiken, T.A., Apkarian, A.V., Porter, K., and Jordan, S.W. (2019). Targeted Muscle Reinnervation Treats Neuroma and Phantom Pain in Major Limb Amputees: A Randomized Clinical Trial. *Ann Surg* 270**,** 238-246.

Farina, D., Vujaklija, I., Sartori, M., Kapelner, T., Negro, F., Jiang, N., Bergmeister, K., Andalib, A., Principe, J., and Aszmann, O.C. (2017). Man/machine interface based on the discharge timings of spinal motor neurons after targeted muscle reinnervation. *Nature Biomedical Engineering* 1**,** 0025.

Gesslbauer, B., Hruby, L.A., Roche, A.D., Farina, D., Blumer, R., and Aszmann, O.C. (2017). Axonal components of nerves innervating the human arm. *Annals of Neurology* 82**,** 396-408.

Guillen, J. (2012). FELASA guidelines and recommendations. *J Am Assoc Lab Anim Sci* 51**,** 311-321.

Hayashi, A., Moradzadeh, A., Hunter, D., Kawamura, D., Puppala, V., Tung, T., Mackinnon, S., and Myckatyn, T. (2007). Retrograde Labeling in Peripheral Nerve Research: It Is Not All Black and White. *Journal of Reconstructive Microsurgery* 23**,** 381-389.

Inciong, J.G., Marrocco, W.C., and Terzis, J.K. (2000). Efficacy of intervention strategies in a brachial plexus global avulsion model in the rat. *Plast Reconstr Surg* 105**,** 2059-2071.

Kapelner, T., Jiang, N., Holobar, A., Vujaklija, I., Roche, A.D., Farina, D., and Aszmann, O.C. (2016). Motor Unit Characteristics after Targeted Muscle Reinnervation. *PLOS ONE* 11**,** e0149772.

Kuiken, T.A., Childress, D.S., and Zev Rymer, W. (1995). The hyper-reinnervation of rat skeletal muscle. *Brain Research* 676**,** 113-123.

Kuiken, T.A., Li, G., Lock, B.A., Lipschutz, R.D., Miller, L.A., Stubblefield, K.A., and Englehart, K.B. (2009). Targeted muscle reinnervation for real-time myoelectric control of multifunction artificial arms. *Jama* 301**,** 619-628.

Mackinnon, S.E., and Novak, C.B. (1999). Nerve transfers. New options for reconstruction following nerve injury. *Hand Clin* 15**,** 643-666, ix.

Mioton, L.M., Dumanian, G.A., Shah, N., Qiu, C.S., Ertl, W.J., Potter, B.K., Souza, J.M., Valerio, I.L., Ko, J.H., and Jordan, S.W. (2020). Targeted Muscle Reinnervation Improves Residual

Limb Pain, Phantom Limb Pain, and Limb Function: A Prospective Study of 33 Major Limb Amputees. *Clin Orthop Relat Res* 478**,** 2161-2167.

Muceli, S., Bergmeister, K.D., Hoffmann, K.P., Aman, M., Vukajlija, I., Aszmann, O.C., and Farina, D. (2019a). Decoding motor neuron activity from epimysial thin-film electrode recordings following targeted muscle reinnervation. *J Neural Eng* 16**,** 016010.

Muceli, S., Poppendieck, W., Hoffmann, K.P., Dosen, S., Benito-Leon, J., Barroso, F.O., Pons, J.L., and Farina, D. (2019b). A thin-film multichannel electrode for muscle recording and stimulation in neuroprosthetics applications. *J Neural Eng* 16**,** 026035.

Muceli, S., Poppendieck, W., Negro, F., Yoshida, K., Hoffmann, K.P., Butler, J.E., Gandevia, S.C., and Farina, D. (2015). Accurate and representative decoding of the neural drive to muscles in humans with multi-channel intramuscular thin-film electrodes. *J Physiol* 593**,** 3789-3804.

Oberlin, C., Béal, D., Leechavengvongs, S., Salon, A., Dauge, M.C., and Sarcy, J.J. (1994). Nerve transfer to biceps muscle using a part of ulnar nerve for C5-C6 avulsion of the brachial plexus: anatomical study and report of four cases. *J Hand Surg Am* 19**,** 232-237.

Percie Du Sert, N., Hurst, V., Ahluwalia, A., Alam, S., Avey, M.T., Baker, M., Browne, W.J., Clark, A., Cuthill, I.C., Dirnagl, U., Emerson, M., Garner, P., Holgate, S.T., Howells, D.W., Karp, N.A., Lazic, S.E., Lidster, K., Maccallum, C.J., Macleod, M., Pearl, E.J., Petersen, O.H., Rawle, F., Reynolds, P., Rooney, K., Sena, E.S., Silberberg, S.D., Steckler, T., and Würbel, H. (2020). The ARRIVE guidelines 2.0: Updated guidelines for reporting animal research. *PLOS Biology* 18**,** e3000410.

Ray, W.Z., Chang, J., Hawasli, A., Wilson, T.J., and Yang, L. (2016). Motor Nerve Transfers. *Neurosurgery* 78**,** 1-26.

Salminger, S., Sturma, A., Hofer, C., Evangelista, M., Perrin, M., Bergmeister, K.D., Roche, A.D., Hasenoehrl, T., Dietl, H., Farina, D., and Aszmann, O.C. (2019). Long-term implant of intramuscular sensors and nerve transfers for wireless control of robotic arms in above-elbow amputees. *Science Robotics* 4**,** eaaw6306.

Scholz, T., Krichevsky, A., Sumarto, A., Jaffurs, D., Wirth, G., Paydar, K., and Evans, G. (2009). Peripheral Nerve Injuries: An International Survey of Current Treatments and Future Perspectives. 25**,** 339-344.

Terzis, J.K., and Papakonstantinou, K.C. (2000). The surgical treatment of brachial plexus injuries in adults. *Plast Reconstr Surg* 106**,** 1097-1122; quiz 1123-1094.

Van Zyl, N., Hill, B., Cooper, C., Hahn, J., and Galea, M.P. (2019). Expanding traditional tendon-based techniques with nerve transfers for the restoration of upper limb function in tetraplegia: a prospective case series. *The Lancet* 394**,** 565-575.

12 Rich Media

Video 1: Grooming behavior 12 weeks following double nerve transfer in the right upper limb.

Video 2: Muscle response upon crushing the motor branch of the long head of the biceps.

Video 3: Muscle response upon ulnar nerve crush following double nerve transfer.

Video 4: Muscle response upon anterior interosseus nerve crush following double nerve transfer.